

# A CLASSICAL DESIGN OF HIGH STEP UP DC-DC CONVERTER FOR RENEWABLE ENERGY APPLICATIONS

Ashadapu. Naresh S <sup>1</sup>, T. Praveen Kumar<sup>2</sup>

<sup>1</sup> Student, Electrical and Electronics Engineering, Jyothismathi institute of technology & science, Telangana, India

<sup>2</sup> Assoc.Prof, Electrical and Electronics Engineering, Jyothismathi institute of technology & science, Telangana, India

## ABSTRACT

*This project, along with the voltage multiplier chain with dual coil output to the boost converter provides a novel parallel input. On the one hand, and to take part in the input current and to reduce input current ripple in the two coils in parallel with the primary windings connected. On the other hand, it is proposed to change, and a series of interleaved output capacitors profit profitable high-voltage, low output voltage ripple, low pressure switch is connected with trying gets. In addition, the two sides increase connected to the secondary coil of the two primary currents parallel to increase the voltage balance between the productive diode and capacitor is coupled in series. In addition, activation key to the current zero level are being driven and connected inductors reasonable inductance leakage diodes to reduce the problem of reverse recovery.*

**Keyword:** - DC-DC converter, dual coupled inductors, high gain, input-parallel output-series, Solar PV System

## 1. INTRODUCTION

high voltage gain dc-dc converters are required in many industrial applications, For example, photovoltaic energy conversion systems and fuel-cell systems usually need high step up and large input current dc-dc converters to boost low voltage (18–56 V) to high voltage (200–400 V) for the grid-connected inverters. High-intensity discharge lamp ballasts for automobile headlamps call for high voltage gain dc-dc converters to raise a battery voltage of 12 V up to 100 V at steady operation [8], [9]. Also, the low battery voltage of 48 V needs to be converted to 380 V in the front-end stage in some uninterruptible power supplies and telecommunication systems by high step-up converters [10], [11]. Theoretically, a basic boost converter can provide infinite voltage gain with extremely high duty ratio. In practice, the voltage gain is limited by the parasitic elements of the power devices, inductor and capacitor. Moreover, the extremely high duty cycle operation may induce serious reverse-recovery problem of the rectifier diode and large current ripples, which increase the conduction losses. On the other hand, the input current is usually large in high output voltage and high power conversion, but low-voltage-rated power devices with small on-resistances may not be selected since the voltage stress of the main switch and diode is, respectively, equivalent to the output voltage in the conventional boost converter.

Many single switch topologies based on the conventional boost converter had been presented for high step-up voltage gain [11]–[15]. The cascaded boost converter is also capable of providing high voltage gain without the penalty of extreme duty cycle [16]. However, the voltage stress of the main switch is equal to the output voltage. In [17] and [18], several switching capacitor/switching-inductor structures are proposed, and transformerless hybrid dc-dc converters with high voltage gain are derived by the use of structures integrated with classical single switch non-isolated PWM converters. They present the following advantage: the energy in the magnetic elements is low, which leads to weight, size, and cost saving for the inductor, and less conduction losses. Another method for achieving high step-up gain is the use of the voltage-lift technique [19], showing the advantage that the voltage stress across the switch is low. However, several diode-capacitor stages are required when the conversion ratio is very large, which makes the circuit complex. In addition, the single switch may suffer high current for high power

applications, which risks reducing its efficiency. Another alternative single switch converters including forward, fly-back and tapped-inductor boost can achieve high conversion ratio by adjusting the turns ratio of the transformer [20]–[22], but these converters require large transformer turns ratio to achieve high voltage gain. In [23], an integrated boost flyback converter is proposed to achieve high voltage gain, and the energy of a leakage inductor is recycled into the output during the switch-off period. Unfortunately, the input current is pulsed from the experimental results. In addition, it should be noticed that the low-level input voltages usually cause large input currents and current ripples to flow through the single switch for high step up and high power dc–dc conversion, which also leads to increasing conduction losses. Therefore, the single-switch topologies are not perfect candidates for high step up dc–dc conversion.

In order to handle high input currents and reduce current ripples, the three-state switching cell based on interleaved control is introduced in boost converters [24]. However, the voltage gain of the conventional three-state switching boost converter is only determined by the duty ratio [18]–[25]. Moreover, the voltage stresses of the power devices are still equivalent to output voltage. Thus, the large duty ratios, high switch voltage stresses, and serious output diode reverse recovery problem are still major challenges for high step up and high power conversion with satisfactory efficiency. To solve aforementioned drawbacks, some three-state switching converters with high static gain employing diode–capacitor cells were presented [25]. However, several diode–capacitor cells are required to meet a very high step-up gain. Thus, other topologies using three-state switching cell and coupled inductors are investigated in [26]–[31]. The authors in [27] proposed an interleaved boost converter with coupled inductors and a voltage doubler rectifier in order to satisfy the high step-up applications and low input current ripple, in which the secondary sides of two coupled inductors are connected in series. The winding-cross-coupled inductors and output diode reverse-recovery alleviation techniques are also introduced in an interleaved three-state switching—dc–dc converters [32], [33], which can get a considerably high voltage conversion ratio and improve the performance of the converter. In [34], an interleaved fly-back converter based on three-state switching cell for high step up and high power conversion is proposed. Although the converter can eliminate the main limitations of the standard fly back, this circuit is a little complex and the input current ripples are large from the experimental results.

This paper proposes an input-parallel output-series boost converter with dual coupled inductors for high step up and high power applications. This configuration inherits the merits of high voltage gain, low output voltage ripple, and low voltage stress across the power switches. Moreover, the presented converter is able to turn ON the active switches at zero current and alleviate the reverse recovery problem of diodes by reasonable leakage inductances of the coupled inductors. A solar Photovoltaic system is used at the input of the proposed converter.

## 2. PHOTOVOLTAIC ARRAY

PV array's output current-voltage curve reflects PV array's dependence on environmental conditions such as ambient temperature and illumination level. Typically, the illumination level ranges from 0 to 1100Wb/m<sup>2</sup> and the temperature range is between 233 and 353 K. Normally, we select 1100 and 298 as the reference values for illumination level and temperature respectively. The relationship between PV array's output characteristics and environmental conditions could be illustrated from general simulation results of PV array. PV array's output power is increased as illumination level increases, while PV array's output power is improved with the decrease of the ambient temperature. The equivalent circuit of a typical pv-cell is given below.

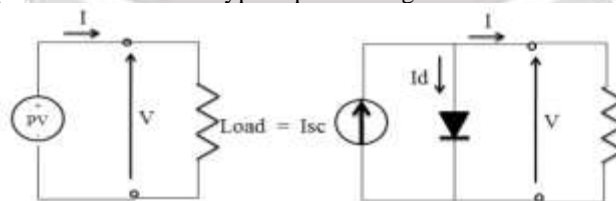


**Fig-1:** Equivalent circuit of photovoltaic cell

Figure reflects a simple equivalent circuit of a photovoltaic cell. The current source which is driven by sunlight is connected with a real diode in parallel. In this case, PV cell presents a p-n junction characteristic of the real diode. The forward current could flow through the diode from p-side to n-side with little loss. However, if the current flows in reverse direction, only little reverse saturation current could get through. All the equations for modelling the PV array are analysed based on this equivalent circuit.

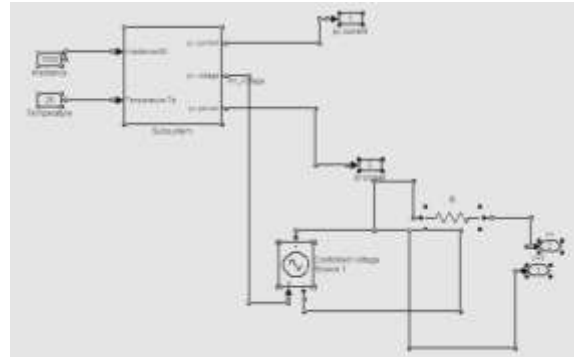


**Fig-2:** Mat lab model of single pv-cell

Boost power converters have been widely used for Power Factor Correction (PFC) in AC-DC conversion and for power management in battery powered DC-DC conversions. Moving beyond low-power applications, such as cellular phones, smart phones and other portable electronic products, boost converters are being used more and more in medium-power applications. For example, in computing and consumer electronics, boost converter-based LED drivers for notebook displays, LCD TVs and monitors have been developed. In communications and industrial products, simple boost converters are used in satellite dish auxiliary power supplies and peripheral card supplies. As boost converters run to CCM (Continuous Conduction Mode), a complex pole pair and a Right-Half Plane (RHP) zero will present in the dynamic characteristic. Some applications of boost converter:

- Programmable soft turn-on for inrush current control
- Hiccup mode for over-current protection
- Complete shutdown with source-load separation
- Simple loop compensation
- Protection for power MOSFET ( $Q_2$ ) failure

### 3. TOPOLOGY AND OPERATION PRINCIPLE OF THE PROPOSED CONVERTER

The proposed topology is shown in Fig. 1. This circuit can be divided as two parts. These two segments are named a modified interleaved boost converter and a voltage doubler module using capacitor–diode and coupled inductor technologies. The basic boost converter is another boost version with the same function in which the output diode is placed on the negative dc-link rail. A modified interleaved boost converter, which is an input-parallel and output-series configuration derived from two basic boost types. Therefore, this part based on interleaved control has several main functions: 1) it can obtain double voltage gain of the conventional interleaved boost; 2) low output voltage ripple due to the interleaved series connected capacitors; and 3) low switch voltage stresses.

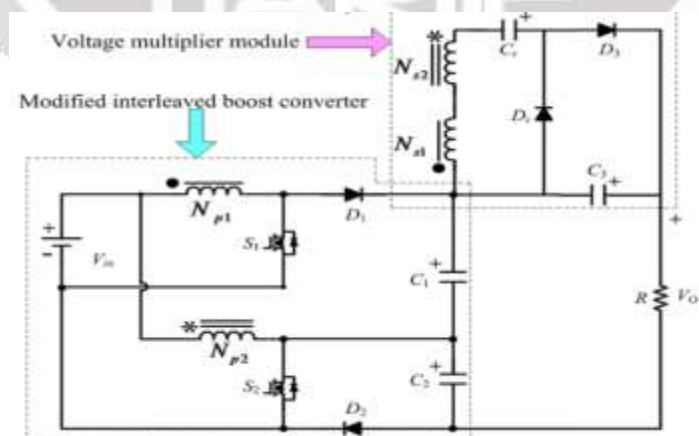


**Fig-3 :** The proposed high gain input-parallel output-series dc/dc converter with dual coupled inductors

- 1) **First stage  $[t_0 - t_1]$ :** At  $t = t_0$ , the power switch  $S_1$  is turned on with zero-current switching (ZCS) due to the leakage inductance  $L_{k1}$ , while  $S_2$  remains turned ON, as shown in Fig. 4. Diodes  $D_1, D_2$ , and  $D_r$  are turned OFF, and only output diode  $D_3$  is conducting. The current falling rate through the output diode  $D_3$  is controlled by the

leakage inductances  $L_{k1}$  and  $L_{k2}$ , which alleviates the diode's reverse recovery problem. This stage ends when the current through the diode  $D_3$  decreases to zero.

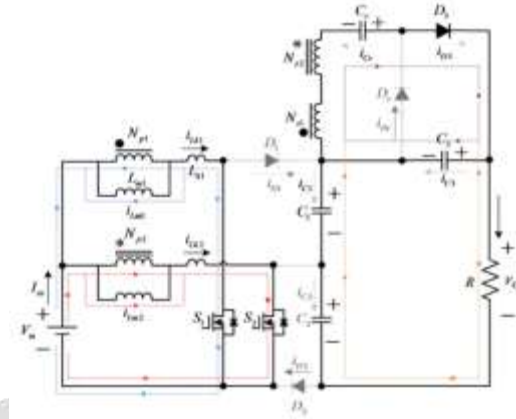


Fig-4: First stage

2) **Second stage**  $[t_1 - t_2]$ : During this interval, both the power switches  $S_1$  and  $S_2$  are maintained turned ON, as shown in Fig. 5 All of the diodes are reversed-biased. The magnetizing inductances  $L_{m1}$  and  $L_{m2}$  as well as leakage inductances  $L_{k1}$  and  $L_{k2}$  are linearly charged by the input voltage source  $V_{in}$ . This period ends at the instant  $t_2$ , when the switch  $S_2$  is turned OFF.

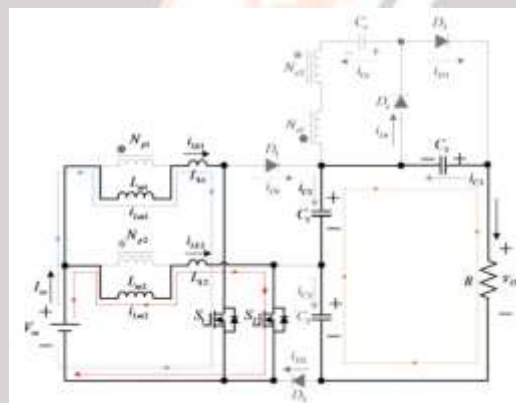


Fig-5: Second stage

3) **Third stage**  $[t_2 - t_3]$ : At  $t = t_2$ , the switch  $S_2$  is turned OFF, which makes the diodes  $D_2$  and  $D_r$  turned ON. The current flow path is shown in Fig. 6. The energy that magnetizing inductance  $L_{m2}$  has stored is transferred to the secondary side charging the capacitor  $C_r$  by the diode  $D_r$ , and the current through the diode  $D_r$  and the capacitor  $C_r$  is determined by the leakage inductances  $L_{k1}$  and  $L_{k2}$ . The input voltage source, magnetizing inductance  $L_{m2}$  and leakage inductance  $L_{k2}$  release energy to the capacitor  $C_2$  via diode  $D_2$ .

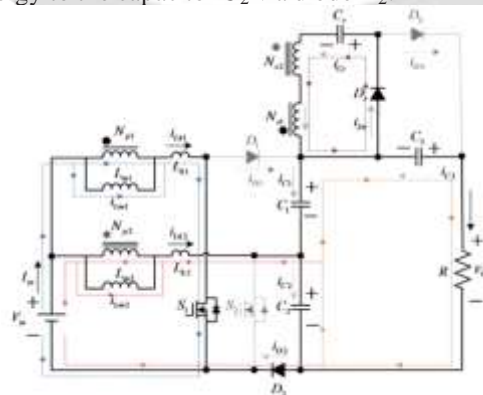


Fig-6: Third stage

4) **Fourth stage** [ $t_3 - t_4$ ]: At  $t = t_3$ , diode  $D_2$  automatically switches OFF because the total energy of leakage inductance  $L_{k2}$  has been completely released to the capacitor  $C_2$ . There is no reverse recovery problem for the diode  $D_2$ . The current-flow path of this stage is shown in Fig. 7. Magnetizing inductance  $L_{m2}$  still transfers energy to the secondary side charging the capacitor  $C_r$  via diode  $D_r$ . The current of the switch  $S_1$  is equal to the summation of the currents of the magnetizing inductances  $L_{m1}$  and  $L_{m2}$ .

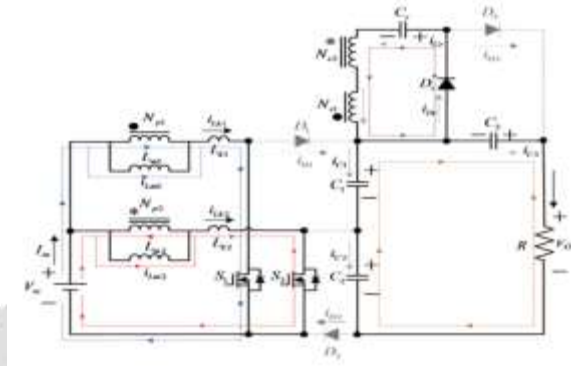


Fig-7: Fourth stage

5) **Fifth stage** [ $t_4 - t_5$ ]: At  $t = t_4$ , the switch  $S_2$  is turned ON with ZCS soft-switching condition. Due to the leakage inductance  $L_{k2}$  and the switch  $S_1$  remains in ON state. The current flow path of this stage is shown in Fig. 8. The current falling rate through the diode  $D_r$  is controlled by the leakage inductances  $L_{k1}$  and  $L_{k2}$ , which alleviates the diode reverse recovery problem. This stage ends when the current through the diode  $D_r$  decreases to zero at  $t = t_5$ .

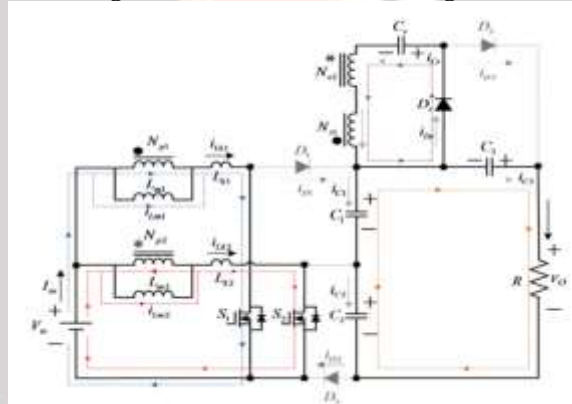


Fig-8: Fifth stage

6) **Sixth stage** [ $t_5 - t_6$ ]: The operating states of stages 6 and 2 are similar. During this interval, all diodes are turned OFF. The magnetizing inductances  $L_{m1}$  and  $L_{m2}$  are the leakage inductances  $L_{k1}$  and  $L_{k2}$  are charged linearly by the input voltage. The voltage stress of  $D_1$  is the voltage on  $C_1$ , and the voltage stress of  $D_2$  is the voltage on  $C_2$ . The voltage stress of  $D_r$  is equivalent to the voltage on  $C_r$ , and the voltage stress of  $D_3$  is the output voltage minus the voltages on  $C_1$  and  $C_2$  and  $C_r$ .

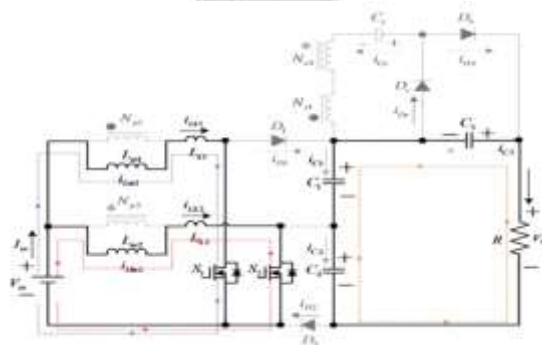


Fig-9: Sixth stage

7) **Seventh stage** [ $t_6 - t_7$ ]: The power switch  $S_1$  is turned OFF at  $t = t_6$ , which turns ON  $D_1$  and  $D_3$ , and the switch  $S_2$  remains in conducting state. The current-flow path of this stage is shown in Fig. 10. The input voltage source  $V_{in}$ , magnetizing inductance  $L_{m1}$  and leakage inductance  $L_{k1}$  release their energy to the capacitor  $C_1$  via the switch  $S_2$ . Simultaneously, the energy stored in magnetizing inductor  $L_{m1}$  is transferred to the secondary side. The current through the secondary sides in series flows to the capacitor  $C_3$  and load through the diode  $D_3$ .

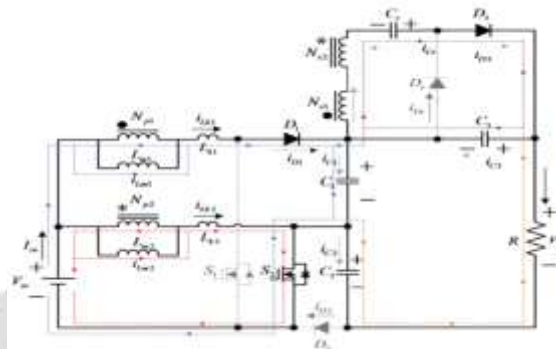


Fig-10: Seventh stage

8) **Eighth stage** [ $t_7 - t'_0$ ]: At  $t = t_7$ , since the total energy of leakage inductance  $L_{k1}$  has been completely released to the capacitor  $C_1$ , diode  $D_1$  automatically switches OFF. The current of the magnetizing inductance  $L_{m1}$  is directly transferred to the output through the secondary side of coupled inductor and  $D_4$  until  $t'_0$ .

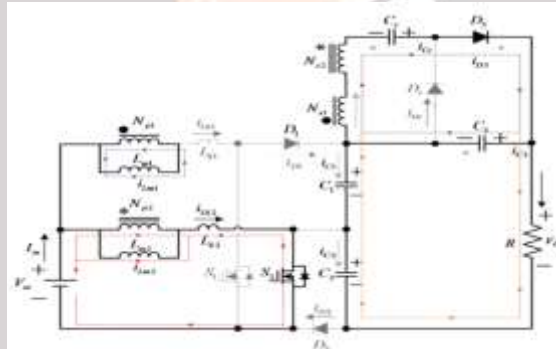


Fig-11: Eighth stage

### 3. APPLICATIONS OF HIGH GAIN BOOST CONVERTER

The dc-dc boost converters are used to convert the unregulated dc input to a controlled dc output at a desired voltage level. They generally perform by applying a dc voltage across an inductor or transformer a period of time (usually in the 20 kHz to 5 MHz range) which causes current to flow through it and store energy magnetically, then switching this voltage off and causing the stored energy to be transferred to the voltage output in a controlled manner. The output voltage is regulated by adjusting the ratio of on/off time.

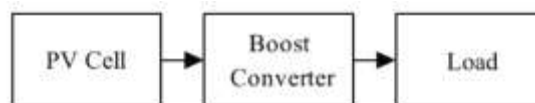
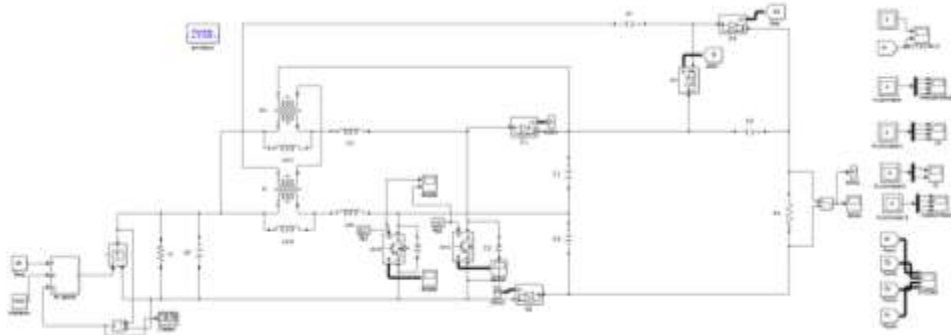


Fig-12: Block diagram

### 4. RESULTS AND ANALYSIS

The proposed system is designed in MATLAB/SIMULINK software. The figures 13 to 20 are results of the proposed circuit. The fig-15, 16 & 17 show the input voltage verses output voltage, voltage across and current through the elements of the proposed circuit.



**Fig-13:** Circuit iagram of proposed circuit using MATLAB

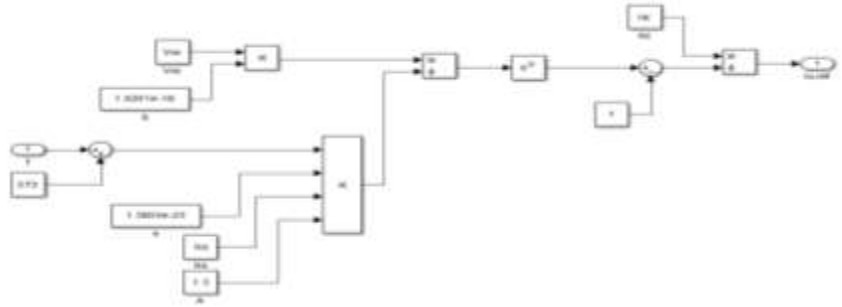


**Fig-14:** Internal circuit of Solar PV System

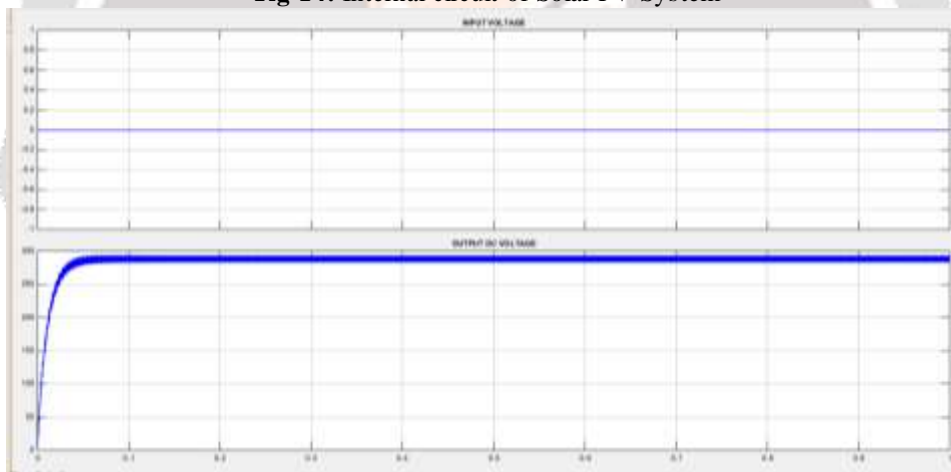


**Fig-15:** input-output voltages of proposed circuit

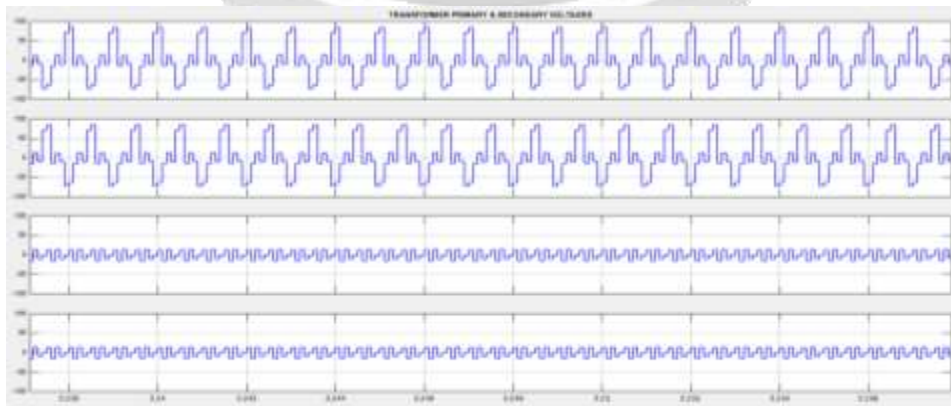


**Fig-16:** Transformer primary and secondary voltages and currents

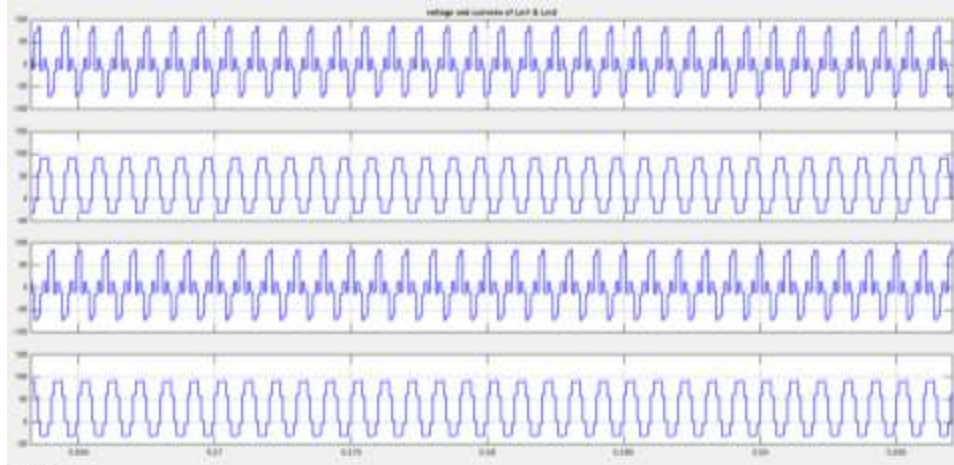


**Fig-17:** The voltage across and current through the Lm1 and Lm2

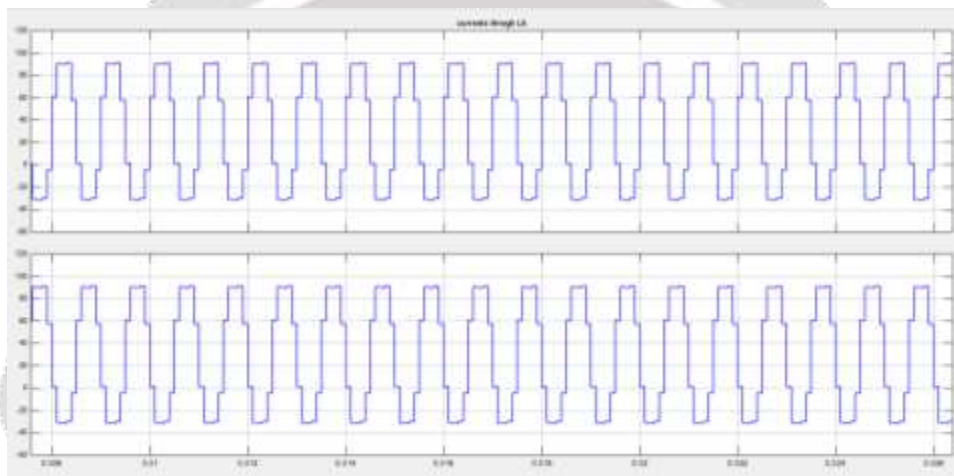


**Fig-18:** The currents through the Lk

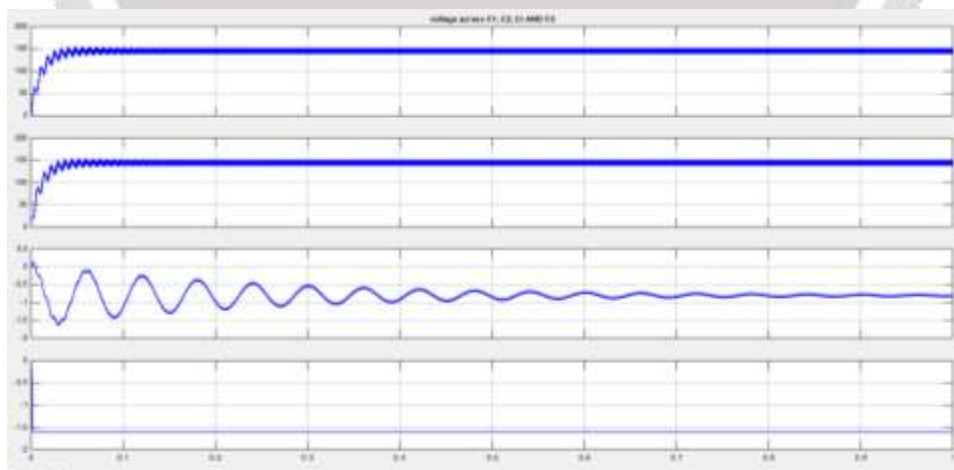


**Fig-19:** The voltage across capacitors c1, c2, Cr, CO





**Fig-20:** The voltage across and current through the diodes.

## 5. CONCLUSION

In the project of “A high gain input-parallel output-series dc/dc converter with dual coupled inductor”. A high gain can be achieved by parameters like duty cycle gate control. By using dual coupled inductor, different switching topologies circuit operation is analyzed. Inductances are connected in parallel, capacitors are connected in series. Inductors, capacitors reduce ripples in output current and output voltage. For low input-voltage and high step up power conversion, this paper has successfully developed a high-voltage gain dc–dc converter by input-parallel output-series and inductor techniques. The key theoretical waveforms with SOLAR PV as input under steady-state operational principle and the main circuit performance are discussed to explore the advantages of the proposed converter Matlab simulink software.

## 6. REFERENCES

- [1] C.Cecati, F. Ciancetta, and P. Siano, “A multilevel inverter for photovoltaic systems with fuzzy logic control,” *IEEE Trans. Ind. Electron.*, vol. 57, no. 12, pp. 4115–4125, Dec. 2010.
- [2] X. H. Yu, C. Cecati, T. Dillon, and M. G. Simoes, “The new frontier of smart grid,” *IEEE Trans. Ind. Electron. Mag.*, vol. 15, no. 3, pp. 49–63, Sep. 2011.
- [3] G. Fontes, C. Turpin, S. Astier, and T. A. Meynard, “Interactions between fuel cell and power converters: Influence of current harmonics on a fuel cell stack,” *IEEE Trans. Power Electron.*, vol. 22, no. 2, pp. 670–678, Mar. 2007.
- [4] J. Y. Lee and S. N. Hwang, “Non-isolated high-gain boost converter using voltage-stacking cell,” *Electron. Lett.*, vol. 44, no. 10, pp. 644–645, May 2008.
- [5] Z. Amjadi and S. S. Williamson, “Power-electronics-based solutions for plug-in hybrid electric vehicle energy storage and management systems,” *IEEE Trans. Ind. Electron.*, vol. 57, no. 2, pp. 608–616, Feb. 2010.
- [6] L. Henrique, S. C. Barreto, P. P. Praca, D. S. Oliveira Jr., and R. N. A. L. Silva, “High-voltage gain boost converter based on three-state commutation cell for battery charging using PV panels in a single conversion stage,” *IEEE Trans. Power Electron.*, vol. 29, no. 1, pp. 150–158, Jan. 2014.
- [7] F. Boico, B. Lehman, and K. Shujaee, “Solar battery chargers for NiMH batteries,” *IEEE Trans. Power Electron.*, vol. 22, no. 5, pp. 1600–1609, Sep. 2007.
- [8] A. Reatti, “Low-cost high power-density electronic ballast for automotive HID lamp,” *IEEE Trans. Power Electron.*, vol. 15, no. 2, pp. 361–368, Mar. 2000.
- [9] A. I. Bratcu, I. Munteanu, S. Bacha, D. Picault, and B. Raison, “Cascaded DC-DC converter photovoltaic systems: Power optimization issues,” *IEEE Trans. Ind. Electron.*, vol. 58, no. 2, pp. 403–411, Feb. 2011.
- [10] H. Tao, J. L. Duarte, and M. A. M. Hendrix, “Line-interactive UPS using a fuel cell as the primary source,” *IEEE Trans. Ind. Electron.*, vol. 55, no. 8, pp. 3012–3021, Aug. 2008.
- [11] Y. P. Hsieh, J. F. Chen, T. J. Liang, and L. S. Yang, “Novel high step-up DC-DC converter for distributed generation system,” *IEEE Trans. Ind. Electron.*, vol. 60, no. 4, pp. 1473–1482, Apr. 2013.
- [12] M. H. Todorovic, L. Palma, and P. N. Enjeti, “Design of a wide input range dc–dc converter with a robust power control scheme suitable for fuel cell power conversion,” *IEEE Trans. Ind. Electron.*, vol. 55, no. 3, pp. 1247–1255, Mar. 2008.

- [13] R. J. Wai, C. Y. Lin, C. Y. Lin, R. Y. Duan, and Y. R. Chang, "High efficiency power conversion system for kilowatt-level stand-alone generation unit with low input voltage," *IEEE Trans. Ind. Electron.*, vol. 55, no. 10, pp. 3702–3714, Oct. 2008.
- [14] S. K. Changchien, T. J. Liang, J. F. Chen, and L. S. Yang, "Novel high step up dc-dc converter for fuel cell energy conversion system," *IEEE Trans Ind. Electron.*, vol. 57, no. 6, pp. 2007–2017, Jun. 2010.
- [15] S. Chen, T. Liang, L. Yang, and J. Chen, "A cascaded high step-up dc-dc converter with single switch for microsource applications," *IEEE Trans. Power Electron.*, vol. 26, no. 4, pp. 1146–1153, Apr. 2011.
- [16] S. V., J. P. F., and Y. L., "Optimization and design of a cascaded DC/DC converter devoted to grid-connected photovoltaic systems," *IEEE Trans. Power Electron.*, vol. 27, no. 4, pp. 2018–2027, Apr. 2012.
- [17] B. Axelrod, Y. Berkovich, and A. Ioinovici, "Switched-capacitor/switched-inductor structures for getting transformerless hybrid dc-dc PWM converters," *IEEE Trans. Circuits Syst. I, Reg. Papers*, vol. 55, no. 2, pp. 687–696, Mar. 2008.
- [18] M. Prudente, L. L. Pfitscher, G. Emmendoerfer, E. F. Romaneli, and R. Gules, "Voltage multiplier cells applied to non-isolated DC-DC converters," *IEEE Trans. Power Electron.*, vol. 23, no. 2, pp. 871–887, Mar. 2008.

